Corrosion and hydrogen permeation of low alloy steel in H2S-containing environments : the effect of test buffer solution chemistry

Martien Duvall Deffo Ayagou, Gaurav Joshi, Bernard Tribollet, Thi Tuyet Mai Tran, Christophe Mendibide, Jean Kittel

Corrosion and hydrogen permeation of low alloy steel in H_2S-containing environments: the effect of test buffer solution chemistry

Martien Duvall Deffo Ayagou[1], Gaurav R. Joshi[2], Bernard Tribollet[3], Thi Tuyet Mai Tran[3], Christophe Mendibide[1] and Jean Kittel[2]

[1]*Institut de la Corrosion, Fraisses, France*
[2]*IFP Energies nouvelles, Solaize, France*
[3]*LISE, Paris, France*

Abstract

H_2S-containing (sour) service environments present a considerable risk of hydrogen induced cracking (HIC) and sulfide stress cracking (SSC) to steel line pipe, pressure vessel and tubular components during upstream oil and gas production, through the ability of H_2S to corrode and promote hydrogen entry into the material bulk via a cathodic reaction process. Materials selection for sour service is made via standard test methods such as NACE TM0284 and NACE TM0177. A commonly used test solution (NACE TM0177 solution A) comprises sodium chloride (5.0%) + acetic acid (0.5%), to work in a range between pH 2.8 – 4.0. When pH stability is essential over long testing periods, solutions that are buffered by acetic acid with sodium acetate are proposed. NACE TM0177 solution B (5.0% NaCl + 0.4% sodium acetate + 2.5% acetic acid) presents an initial pH of 3.4 – 3.6, specified not to exceed pH 4.0 over the testing duration. Newer, alternative solutions from the high-strength line pipe (HLP) research committee from the Iron and Steel Institute of Japan (ISIJ) propose higher acetic acid/acetate concentrations for enhanced buffering capacity. This may offer practical testing advantages, although material corrosion rates and hydrogen uptake are possibly affected.

In this conference proceeding, we report on the corrosion and hydrogen uptake performance of a sour-grade X65 steel exposed to NACE Solutions A and B, and an HLP solution (at the same pH as NACE B solution, i.e. pH 3.5) under continuous H_2S purging (0.1 MPa, T = 24°C) over 720 hours. Electrochemical methods measure electrochemical impedance at the entry face of, and hydrogen permeation across, the X65 membrane. Overall, the differences we note are linked to the different weak acid/conjugate base concentration.

Keywords

Hydrogen permeation, acetic acid, hydrogen sulfide, X65 steel

Introduction

Materials used in oil and gas industries are exposed to H_2S-containing (sour) environments, which is corrosive and known to promote hydrogen entry into steels. This may lead to several types of failures such as hydrogen-induced cracking (HIC), sulfide stress cracking (SSC), or stress-oriented hydrogen induced cracking (SOHIC). Standard test methods have been developed for the selection and the qualification of steels for use in H_2S containing environments, such as NACE TM0177 and TM0284 [1; 2]. Selecting test conditions for carbon and low alloy steel qualification is conducted using a pH(y)-P_{H2S}(x) diagram to impose 'levels of severity' for assessing material cracking susceptibility [3]. It is, nonetheless, acknowledged that the solution chemistry may affect the test result [4]. The prescribed solutions in the current ISO15156 standard contain 5% NaCl with acetic acid (CH_3COOH or HAc)/sodium acetate (CH_3COONa or NaAc) buffered to fix the solution pH over a long testing period (720 h) [3]. Born out of a need to use a test solution with excellent pH stability for fitness for purpose (FFP) HIC tests, the high-strength line pipe (HLP) research committee from the Iron and Steel Institute of Japan (ISIJ) proposed higher HAc + NaAc concentrations for enhanced buffering capacity [5–7]. In this conference proceeding, we expose a sour-service grade X65 to NACE A, NACE B and ISIJ HLP solutions saturated with H_2S (P_{total} and P_{H2S} ~1 bar) for a period of 720 h. Both corrosion and hydrogen uptake tests have been conducted using a classic two-chamber hydrogen permeation cell in order to evaluate the influence on the solution chemistry on material performance.

Experimental procedure

Solution chemistry

Test solutions, NACE A (pH_{start} = 2.7) and B (pH_{start} = 3.5) representative of qualification tests (e.g. NACE TM0177), and an ISIJ HLP solution at the same pH as NACE B (pH_{start} = 3.5) were used. The solution compositions are provided in Table 1. In addition, results in an unbuffered 3.5 wt% NaCl solution (pH = 4.3) are sometimes included for comparative purposes.

Table 1: Acetate concentration used in test solutions in this work (T = 24°C, P_{H2S} ~1 bar, t = 720 h).

	Composition	$[HAc]_{(aq)}$ (M)	$[NaAc]_{(aq)}$ (M)	$[Ac^-]_{(aq)}$ (M)
NACE A	0.5% HAc	0.09		0.09
NACE B	2.5% HAc + 0.4% NaAc	0.42	0.05	0.47
HLP	5.0% HAc + 0.8% NaAc	0.83	0.1	0.93

Corrosion and hydrogen permeation tests

Exposure of X65 steel specimens was carried out in a jacketed Devanathan-Stachurski cell [8]. The solution temperature was maintained at 24 +/- 2°C, through circulating thermally-controlled water through the cell's jackets. The iron/steel membrane was used for two distinct types of electrochemical measurements, carried out simultaneously. EIS measurements were performed at the charging side left at the free corrosion potential (E_{corr}). At the same time, the exit surface of the membrane covered with a Pd deposit was held in a deoxygenated 0.1 M NaOH solution and polarized at a potential of +250 mV vs. Hg/HgO (1M KOH) providing a direct measurement of the hydrogen flux across the steel membrane. Membrane thickness was 0.5 mm, and the exposed area was 16.6 cm² on both sides. In addition to the permeation

membrane, weight-loss specimens of the same material as the permeation membrane (9 mm x 9 mm x 0.5 mm) were also introduced into the charging cell. These coupons were used for weight-loss corrosion rate evaluation. Accounting for the surface areas of the permeation membrane and iron coupons, the ratio between test solution volume and exposed surface was close to 30 mL/cm². The continuous H_2S gas bubbling in the charging cell provides the only source of solution convection.

Results and discussion

Impact of buffer choice on solution pH

Figure 1 shows the results of the buffer solution pH as a function of time over 720h. For the test configuration employed, both NACE B and the HLP solution provide an excellent pH stability close to pH 3.5 over the 720 h exposure period.

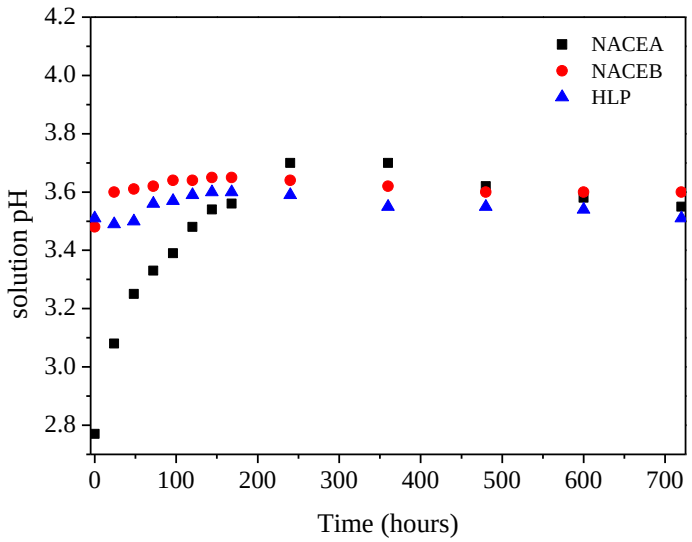

Fig 1: Evolution of test solution pH as a function of time over 720 h (T = 24°C, P_{H2S} ~1 bar).

Impact of acetate concentration on corrosion

The evolution of corrosion rates (Fig 2(a)) is derived from the corrosion current, i_{corr} using R_{ct} and the anodic Tafel coefficient of b_a = 40 mV dec^{-1}, with 7.8 g/cm^3 as the steel density. This is justified in [9].

$$\boldsymbol{i_{corr} = b_a/2.3\ R_{ct}} \qquad \textbf{(1)}$$

Electrochemical corrosion rate data are supported by coupon mass loss corrosion rates in Fig. 2(b), which also contains integrated EIS corrosion rates for comparison.

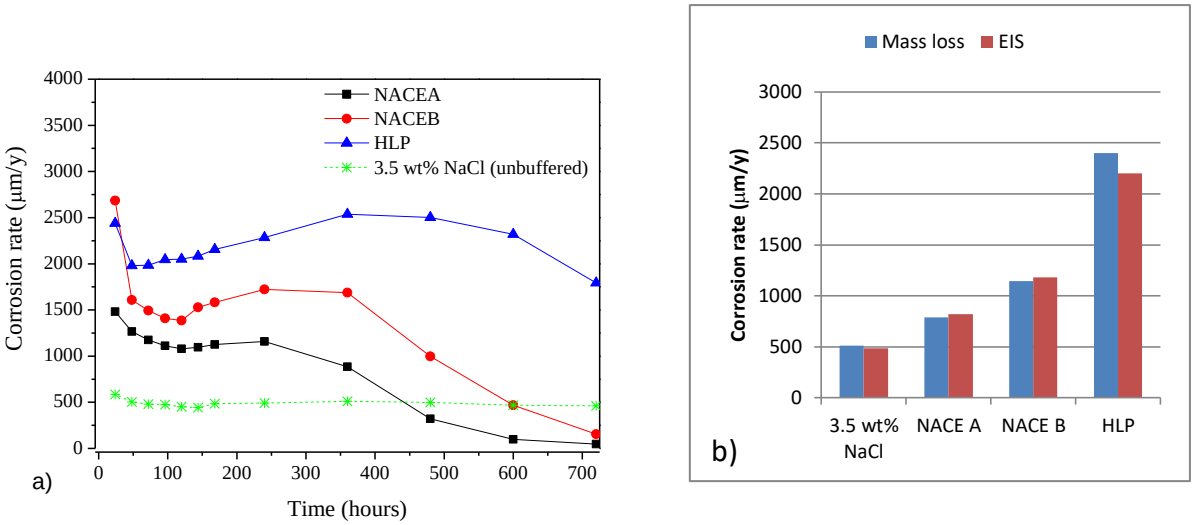

Fig. 2: Time evolution of the corrosion rate obtained from electrochemical measurements (a) and average corrosion rates determined from mass loss and electrochemical measurements (b) of X65 membrane exposed to buffer solutions at T = 24°C under 1 bar H_2S.

A good correlation is obtained between mass loss and electrochemical corrosion rate (CR) estimates throughout the testing campaign, which justifies the choice of b_a = 40 mV dec^{-1} as our chosen anodic Stern-Geary coefficient. Looking at the corrosion rate (CR) evolution in Fig 2(a), it is noted that the CR profiles in NACE solutions are quite similar. X65 corrodes at a higher rate in NACE B relative to NACE A, before quickly decreasing to low values over the final 360 h. These values recorded at the 720th hour are 90% lower than the value recorded at the 360th hour. The CR in HLP solution is sustained at the highest rates, more than two times greater than NACE B, and shows a far slower kinetics of decrease over the final 360 h of immersion (to a final CR that is only 30% lower than its value recorded at the exposure midpoint. This qualitatively implies that a protective iron sulfide overlayer quite possibly forms at the X65 interface only in the NACE solutions. Looking at Figure 2 (b), it appears that for H_2S-saturated *buffered* solutions under the same partial pressure (~1 bar and ~0.1 M H_2S_{aq}), comparable solution pH (3.5 ± 0.2) and hydrodynamics, a higher aqueous acetic acid + acetate concentration ([HAc + Ac^-]) elevates the base CR (i.e. HLP > NACE B > NACE A). Such an effect of acetic acid/acetate concentration on increasing steel corrosion rate has also been reported in the literature. It is possible that a buffering mechanism played by the acetic acid/acetate equilibrium, to supply protons for the cathodic reduction, might be at play to accelerate the X65 corrosion rate [10].

$$\mathbf{CH_3COOH \leftrightarrow CH3COO^- + H^+} \qquad \mathbf{(2)}$$

This dissociation reaction might take place in the diffusion layer or be catalyzed on contact with a cathodic reaction site at the surface. Increasing its concentration would increase the diffusion-limited cathodic current density. Furthermore, the higher acetate anion concentrations in HLP vs NACE B may be relevant, as Ac^- competes with H_2S_{aq} to react with oxidized ferrous ions and form ferrous acetate. This species would remain in a dissolved state due to higher solubility in aqueous media relative to iron sulfides. We summarise the important metal loss corrosion reactions in Equations 3 – 5. We expect that the higher [HAc + NaAc] disrupts the precipitation pathways to the formation of protective iron sulfide, based on the observation of the delayed onset of corrosion rate decrease in the buffered solutions (i.e. HLP > NACE B > NACE A).

$$Fe + H_2S_{aq} \rightarrow FeS_{(s)} + 2H_{ad} \quad (3)$$

$$Fe + CH_3COOH \rightarrow Fe(CH_3COO)_{2\,(aq)} + 2H_{ad} \quad (4)$$

$$Fe^{2+} + 2CH_3COO^- \rightarrow Fe(CH_3COO)_{2\,(aq)} \quad (5)$$

Impact of acetate concentration on hydrogen permeation

Figure 4 shows the hydrogen permeation profiles obtained in the different buffered solutions. After the initial peak in hydrogen permeation (J_{max}), attained within the first hour of exposure (left hand side in Figure 3), the hydrogen uptake decreases. J_{max} values tended to increase with acetic acid concentration.

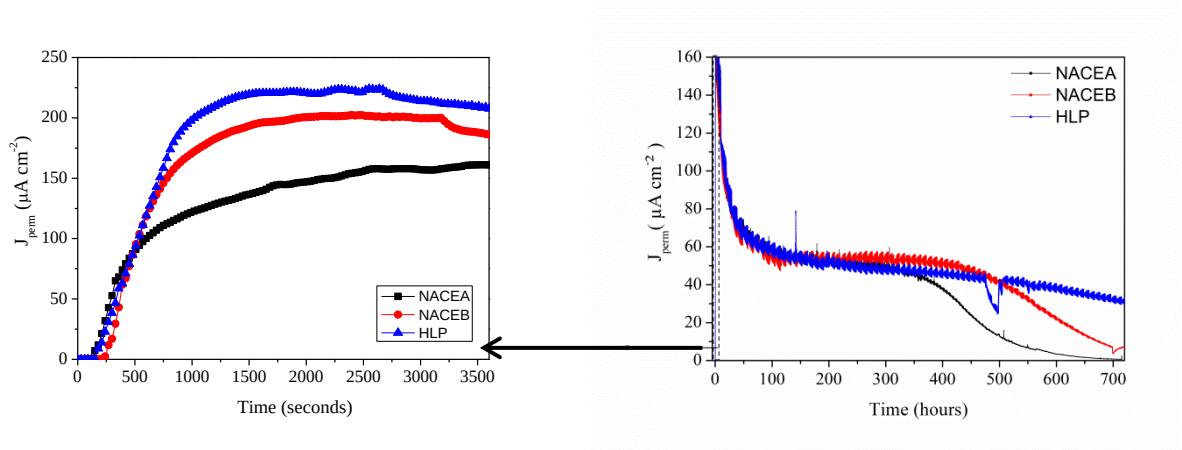

Fig 3: Hydrogen permeation across X65 membrane exposed to buffer solutions at T = 24°C under 1 bar H_2S. The graph on the left shows the very initial peak (J_{max}).

A *quasi*-steady-state is reached by the 120th hour, one governed by surface reaction control (corrosion rate and iron sulfide corrosion product formation at the entry face). Here, the steady state permeation behaviour is within a similar range in all buffered solutions (~55 µA/cm^2) for the subsequent 240 h. Over the final 360 h of exposure, the H-permeation profiles for X65 in the NACE solutions follow the same trend as the EIS corrosion rate evolution, with marked decreases to zero current at similar times. It confirms, for these cases, that hydrogen absorption becomes restricted as the instantaneous CR decreases. For the HLP solution, however, hydrogen permeation is sustained at an appreciable value for the entire duration. It does appear to slowly decrease over the final 240h, in line with the slow decrease in corrosion rates observed for this solution.

The high acetic acid/acetate concentration permits the high corrosion rate, but the involvement of H_2S_{aq} at the steel/solution and scale/solution interface enables the hydrogen permeation to continue at higher fluxes for longer. As Kahyarian *et al* state [10], increasing the concentration of acetic acid may serve simply as an additional source of readily available protons for reduction at the interface. In the absence of H_2S, increasing the acetic acid concentration would simply increase the corrosion rate of iron through the enhanced reduction rates, and through the high solubility of the corrosion product iron acetate (Equation 4). The higher concentration of acetates keeps corroded Fe^{2+} in aqueous form, rather than enabling the precipitation/formation of quite insoluble iron sulfides Fe_xS_y. This could explain the later

onset and slower decrease of the corrosion rates in the buffers with higher HAc, i.e. how X65 corrosion rates in NACE A begin to fall after the 10th day and those in HLP after the 20th day of immersion. In the presence of 0.1M H_2S_{aq}, a high proportion of surface adsorbed hydrogen subsequent to the cathodic corrosion reaction from dissociated acetic acid protons and H_2S protons, will absorb into the subsurface of the X65 steel. Reference to Fig 4 shows that raising the *effective* interfacial proton availability (diffusion-controlled *proton reduction rate*) for the cathodic reaction through an acetic acid buffering mechanism acts to increase the instantaneous hydrogen uptake flux. Considering, further, that the high concentration of acetic acid may dissolve existing FeS, it may very well reduce the overall protective ability of the scale that develops in HLP solution. All these factors together could explain how and why the higher [HAc + Ac^-] maintains the highest and longest hydrogen permeation flux amongst the studied buffer solutions throughout the 30-day exposure period. Our results convey that baseline corrosion rates increase with HAc, but so do the rates of hydrogen permeation – which are maintained at a high level throughout the prescribed testing period. This HLP solution could be an interesting choice in materials testing under hydrogenated environments, if a particularly aggressive and high hydrogen charging medium is sought.

Conclusions

We have conducted a study on the effect of changing the acetic acid and sodium acetate concentration [HAc + NaAc] in a 5% NaCl solution, under continuous H_2S purging (1 bar, T = 24°C) over 720 hours, on the corrosion and hydrogen permeation response of a sour-service grade X65 steel. The tested solutions were The NACE TM0177 solutions NACE A (0.5% HAc), NACE B (2.5% HAc + 0.4% NaAc) and an ISIJ HLP solution (5% HAc + 0.8% NaAc). Our results show that electrochemical and weight loss corrosion rates considerably increase as the total [HAc + NaAc] is increased, likely down to a higher diffusion-controlled cathodic reaction rate from acetic acid/acetate buffering as well as the solubilisation of ferrous ions in the presence of acetate. This latter effect delays the likely formation of a highly protective iron sulfide film on the H-entry surface of X65 steel in HLP and NACE B solutions, if compared against NACE A. The hydrogen permeation flux tracks well with the instantaneous electrochemical corrosion rates, and decreases at similar times. The data suggest that there is significant effect on material in these different buffered media, and care must be taken when selecting a test solution for a given general or FFP test.

References

1. "NACE TM0177-2016: Laboratory testing of metals for resistance to sulfide stress cracking and stress corrosion cracking in H2S environments," NACE International, 2016.
2. "NACE TM0284-2016: Evaluation of pipeline and pressure vessel steels for resistance to hydrogen-induced cracking," NACE International, 2016.
3. ISO 15156-2:2015, "Petroleum and Natural gas industries - Materials for use in H2S-containing environments in oil and gas production - Part 2: Cracking resistant carbon and low alloy steels, and the use of cast iron," (International Organization for Standardization, 2015).
4. K. Kobayashi, T. Omura, H. Amaya, *Corrosion* 74, 7 (2018): p. 788–800.
5. K. Kobayashi, T. Hara, D. Mizuno, N. Ishikawa, E. Tada, "Effect of balance gas on sour corrosion and HIC behavior of carbon steel," Corrosion 2015, 15-19 March (2015).
6. D. Mizuno, N. Ishikawa, T. Hara, K. Kobayashi, E. Tada, "The effect of buffering capacity on HIC behavior for FFP evaluation," Corrosion 2014, Paper 3863, 9-13 March (2014).

7. K. Kobayashi, T. Omura, T. Hara, M. Okatsu, N. Ishikawa, “Proposal of HIC test solution with buffer capacity in NACE TM0284,” Corrosion 2013, 17-21 March (2013).
8. M.A.V Devanathan and Z. Stachurski, *J. Electrochem. Soc.* 111, 5 (1962): p. 619–623.
9. M.D. Deffo Ayagou, T.T. Mai Tran, B. Tribollet, J. Kittel, E. Sutter, N. Ferrando, C. Mendibide, C. Duret-Thual, *Electrochimica Acta* 282 (2018): p. 775–783.
10. Aria Kahyarian, Alex Schumaker, Bruce Brown, Srdjan Nesic, *Electrochimica Acta* 258 (2017): p. 639–652, https://www.sciencedirect.com/science/article/pii/S0013468617324714.